Dynamical effects in line shapes for coupled chromophores: Time-averaging approximation

Cite as: J. Chem. Phys. **127**, 104105 (2007); https://doi.org/10.1063/1.2766943
Submitted: 30 May 2007 . Accepted: 03 July 2007 . Published Online: 12 September 2007

B. M. Auer, and J. L. Skinner

Dynamical effects in line shapes for coupled chromophores: Time-averaging approximation

B. M. Auer and J. L. Skinner
Theoretical Chemistry Institute, University of Wisconsin, Madison, Wisconsin 53706, USA
and Department of Chemistry, University of Wisconsin, Madison, Wisconsin 53706, USA

(Received 30 May 2007; accepted 3 July 2007; published online 12 September 2007)

For an isolated resonance of an isolated chromophore in a condensed phase, the absorption line shape is often more sharply peaked than the distribution of transition frequencies as a result of motional narrowing. The latter arises from the time-dependent fluctuations of the transition frequencies. It is well known that one can incorporate these dynamical effects into line shape calculations within a semiclassical approach. For a system of coupled chromophores, both the transition frequencies and the interchromophore couplings fluctuate in time. In principle one can again solve this more complicated problem with a related semiclassical approach, but in practice, for large numbers of chromophores, the computational demands are prohibitive. This has led to the development of a number of approximate theoretical approaches to this problem. In this paper we develop another such approach, using a time-averaging approximation. The idea is that, for a single chromophore, a motionally narrowed line shape can be thought of as a distribution of time-averaged frequencies. This idea is developed and tested on both stochastic and more realistic models of isolated chromophores, and also on realistic models of coupled chromophores, and it is found that in all cases this approximation is quite satisfactory, without undue computational demands. This approach should find application for the vibrational spectroscopy of neat liquids, and also for proteins and other complicated multichromophore systems. © *2007 American Institute of Physics*. [DOI: 10.1063/1.2766943]

I. INTRODUCTION

Spectroscopy is a powerful tool for probing the structure and dynamics of condensed phase systems.[1–3] Its utility arises from the sensitivity of a chromophore's transition frequencies to its local environment. For example, the vibrational frequency of the OH stretch in water is sensitive to the extent of local hydrogen bonding. Therefore, steady-state and ultrafast vibrational spectroscopy have provided much information about the structure and dynamics of the hydrogen bond network in liquid water.[4] As another example, vibrational spectroscopy is playing an increasingly important role in probing the structure and dynamics of biomacromolecules.[5–16]

In general the transition frequency of a particular vibrational mode of a chromophore in a condensed phase will fluctuate, on some characteristic time scale, due to molecular motions. If this time scale is sufficiently slow, under certain conditions the line shape of the ensemble of chromophores is simply the distribution of frequencies. This is known as the inhomogeneous limit, since on the relevant time scale each member of the ensemble is different. On the other hand, if the time scale of the fluctuations is not sufficiently slow then effects of the fluctuation dynamics appear in the spectrum, and in particular, the line shape is narrower than the distribution of frequencies and is said to be "motionally narrowed." When the frequency fluctuations are very fast (the extreme-narrowing limit), each member of the ensemble is statistically the same (on the relevant time scale), and so the line shape is said to be homogeneously broadened. This phenomenology can be understood from the general semiclassical formula for the absorption line shape of an isolated chromophore.[1,17]

Some time ago Kubo developed a simple stochastic model for the line shape,[18] where the fluctuating frequency describes a Gaussian process, and the two-point time-correlation function decays exponentially. In this special case the problem can be solved analytically. In a more realistic situation, where the frequency fluctuations are not Gaussian and the time-correlation function is not exponential, to calculate the line shape one would run a molecular dynamics simulation, and at each time step compute the transition frequency. Then from the resulting frequency trajectory the line shape can be calculated by using the general semiclassical formula.[1,17] In the above discussion we have implicitly assumed that the magnitude of the transition dipole is independent of local environment (often called the Condon approximation) and have neglected rotations. If these need to be included the semiclassical formula can be generalized.[1,19] The inclusion of non-Condon effects necessitates a calculation of the fluctuating transition dipole (as well as of the transition frequency).[19]

Up until this point the discussion has focused on an "isolated" chromophore (one that is interacting with the solvent but not with any other chromophores). Often, however, one is interested in situations when many chromophores are coupled. For example, if we are dealing with vibrational spectroscopy of a neat molecular liquid, with one vibrational chromophore (in a particular spectral region) per molecule,

these chromophores will interact via intermolecular coupling. Or consider a more complicated situation such as liquid water, where each molecule has two vibrational chromophores (in the OH stretch region), and so there is both intramolecular and intermolecular coupling. Finally, one might consider the vibrational spectroscopy in the amide I region of a protein, where each peptide bond contains one vibrational chromophore, and in general these chromophores are coupled. In any of these cases if the couplings are large enough compared to the differences in the frequencies of the individual chromophores, the instantaneous vibrational eigenstates of the system will become delocalized, possibly over many chromophores. These delocalized states are referred to as exciton states.

Theoretical description of vibrational spectroscopy in this situation is complicated, as the exciton states are changing as time evolves, due to the fluctuating chromophore frequencies and couplings. As in the case of the isolated chromophore, a semiclassical formula for the line shape for a coupled system can be derived, and non-Condon effects can be included if desired.[15,16] Unfortunately the formula is very computationally demanding to evaluate because it involves repeated operations on potentially very large matrices.[20–23] The result is that the algorithm does not scale well and is time consuming to implement, and hence it is often not possible to apply to realistic problems of current interest. To this end a number of further approximations have been developed, which are expected to be useful under certain circumstances. For example, if the couplings are weak one can treat them perturbatively, and if non-Condon effects are not important, one arrives at a semiclassical line shape formula identical in form to that for isolated chromophores, but where each chromophore's frequency has been renormalized by the couplings.[24] If one further makes the cumulant approximation this leads to the familiar result first derived by Oxtoby *et al.*[25] Alternatively, if dynamical effects (motional narrowing, for example) are not important, then one can find the eigenstates exactly for each time step, and average over the resulting distribution.[10,12,26,27] If the number of chromophores is small, and the frequencies and couplings are such that the excitonic eigenstates are always well separated and do not cross, then an adiabatic approximation becomes appropriate.[15,28] If the relative positions of the chromophores do not fluctuate very much, as in the case of a folded protein, then one can use the eigenstates of the average Hamiltonian as a useful reference basis set.[26,29,30] Mukamel and Abramavicius have also developed an alternative approach, formulated in the local chromophore basis set, involving nonlinear exciton equations.[9]

Another alternative approximate approach to including dynamics in calculations of line shapes for coupled chromophores comes from considering the concept of motional narrowing, first for isolated chromophores, from a physical point of view. The idea is that, because of the (correct) mathematics of the semiclassical line shape formula, the full frequency distribution is partially averaged because of dynamics on sufficiently fast time scales. The question then arises, can one obtain a reasonable approximation to the line shape by considering the distribution of time-averaged frequencies, averaged over some appropriate time scale? This approach was put forth some time ago by Ojamäe *et al.*,[31] although in their case they used this to average over *unphysical* fast dynamics caused by treating high-frequency intramolecular vibrations classically. Recently Buch implemented the above idea in her calculations of the water surface,[32] where the OH stretch chromophores (local modes) are coupled, by averaging the local mode frequencies over 1 ps.

In this paper we systematically explore this idea of using a time-averaging approximation (TAA) to incorporate dynamical effects into the calculation of linear spectra of both isolated and coupled chromophores. We begin in Sec. II with the development of the theory of the TAA. We also discuss alternative approaches, such as the adiabatic and effective frequency approximations. In Sec. III A we first implement this approach for the stochastic Kubo model for an isolated chromophore,[18] finding that as long as the averaging time is chosen appropriately the TAA works quite well. We also find the delightfully simple and perhaps surprising result that the appropriate averaging time T is to a good approximation related only to the actual line width Γ, by $T \simeq 5/\Gamma$! In Secs. III B–III E we then test the TAA compared to exact results for realistic model problems involving the OH stretch region of liquid water, both with and without intramolecular coupling, and including or not including non-Condon and rotational effects. In all cases the TAA works reasonably well, and better than other easily implemented approximations. In Sec. IV we conclude.

II. LINE SHAPE THEORY AND TIME-AVERAGING APPROXIMATION

If the electric field of the excitation light is polarized in the $\hat{\boldsymbol{\epsilon}}$ direction, the linear absorption line shape is the Fourier transform of the quantum dipole time-correlation function,

$$I(\omega) \sim \int_{-\infty}^{\infty} dt e^{-i\omega t} \langle \hat{\boldsymbol{\epsilon}} \cdot \boldsymbol{\mu}(0) \boldsymbol{\mu}(t) \cdot \hat{\boldsymbol{\epsilon}} \rangle, \tag{1}$$

where $\boldsymbol{\mu}$ is the dipole operator for the system, and the brackets indicate a quantum equilibrium statistical mechanical average. For an isolated resonance of an isolated chromophore one often makes the two-state approximation, within which the Hamiltonian is written as

$$H = H_0 |0\rangle\langle 0| + H_1 |1\rangle\langle 1|, \tag{2}$$

where $|0\rangle$ is the ground quantum state, $|1\rangle$ is the excited quantum state for the spectroscopic transition of interest, and H_0 and H_1 are the corresponding Hamiltonians that involve all other degrees of freedom. Within this two-state basis the dipole operator can be written without loss of generality as

$$\boldsymbol{\mu} = \boldsymbol{\mu}_1 \{ |0\rangle\langle 1| + |1\rangle\langle 0| \}, \tag{3}$$

where $\boldsymbol{\mu}_1$ is the transition dipole operator. If the transition energy is much larger than kT, within the mixed quantum/classical approach (meaning that H_0, H_1, and $\boldsymbol{\mu}_1$ are replaced at the appropriate time in the derivation by their classical analogues), the line shape becomes[1,17,33]

$$I(\omega) \sim \int_{-\infty}^{\infty} dt e^{-i\omega t} \left\langle m(0)m(t)\exp\left[i\int_0^t dt' \omega(t') \right] \right\rangle, \quad (4)$$

where $m=\boldsymbol{\mu}_1\cdot\hat{\boldsymbol{\epsilon}}$, $\omega(t)$ is the fluctuating transition frequency, and the brackets now indicate a classical equilibrium statistical mechanical average with respect to the ground state Hamiltonian. Lifetime broadening can be included phenomenologically if necessary.

The transition frequency fluctuations can be characterized by their rms deviation Δ, and correlation time τ. If the frequency fluctuations are sufficiently slow, meaning that $\Delta\tau \gg 1$, $\omega(t')$ in Eq. (4) can be replaced by its initial value $\omega(0)$. If in addition $m(t)$ can be replaced by $m(0)$, then the line shape formula becomes

$$I(\omega) \sim \langle m(0)^2 \delta(\omega-\omega(0)) \rangle. \quad (5)$$

Thus the line shape is simply the equilibrium distribution of initial frequencies $\omega(0)$ weighted by the square of the projection of the transition dipole, which, as mentioned earlier, is called the inhomogeneous limit.

In general m can fluctuate due to changes in the magnitude of $\boldsymbol{\mu}_1$ (non-Condon effects), or to changes in the angle $\boldsymbol{\mu}_1$ makes with $\hat{\boldsymbol{\epsilon}}$ (rotations). If non-Condon effects are small and rotations are slow, or simply for illustrative purposes, one can neglect the fluctuations in m, and Eq. (4) then becomes

$$I(\omega) \sim \int_{-\infty}^{\infty} dt e^{-i\omega t} \left\langle \exp\left[i\int_0^t dt' \omega(t') \right] \right\rangle. \quad (6)$$

In the inhomogeneous limit this becomes

$$I(\omega) \sim \langle \delta(\omega-\omega(0)) \rangle, \quad (7)$$

which of course is simply the distribution of frequencies.

If the frequency fluctuations are Gaussian, one can replace (exactly) Eq. (6) by its second-cumulant truncation. Alternatively, if the fluctuations are "small," the second-cumulant truncation is often a good approximation. In either case we have[1]

$$I(\omega) \sim \int_{-\infty}^{\infty} dt e^{-i(\omega-\langle\omega\rangle)t} e^{-g(t)}, \quad (8)$$

where

$$g(t) = \int_0^t dt'(t-t')C(t'), \quad (9)$$

and $C(t)$, the frequency time-correlation function (TCF), is given by

$$C(t) = \langle \delta\omega(0)\delta\omega(t) \rangle, \quad (10)$$

where $\delta\omega(t)=\omega(t)-\langle\omega\rangle$, and $\langle\omega\rangle$ is the average frequency. As discussed above this TCF can be characterized by its initial value $C(0)\equiv\Delta^2$, and correlation time

$$\tau = \int_0^{\infty} dt C(t)/C(0). \quad (11)$$

In the limit $\Delta\tau \gg 1$, $g(t) \simeq \Delta^2 t^2/2$, which leads to a Gaussian line shape whose full width at half maximum (FWHM) is $2\sqrt{2\ln 2}\Delta$. In the limit $\Delta\tau \ll 1$, $g(t) \simeq t\Delta^2\tau$, which leads to a Lorentzian line shape whose FWHM is $2\Delta^2\tau$. Since in this limit this is much smaller than the width of the distribution of frequencies ($2\sqrt{2\ln 2}\Delta$), and this narrowing is due to the dynamics of the frequency fluctuations, this is referred to as motional narrowing. Motional narrowing can also occur when non-Condon effects and rotations are important, but its analysis is more complicated.

Now we turn to the central idea of this paper. We begin by rewriting Eq. (6) as

$$I(\omega) \sim \int_{-\infty}^{\infty} dt e^{-i\omega t} \left\langle \exp\left[it\frac{1}{t}\int_0^t dt' \omega(t') \right] \right\rangle. \quad (12)$$

This can be interpreted as a system oscillating with an effective frequency $(1/t)\int_0^t dt'\omega(t')$, which is just the frequency averaged over time period t. This is consistent with the physical idea that motional narrowing comes about because of self-averaging due to fast frequency fluctuations. Perhaps one can arrive at an approximate expression for the line shape that involves replacing the above frequency, averaged over time t, with a frequency averaged over some fixed time T, to be suitably chosen! Defining

$$\omega_T = \frac{1}{T}\int_0^T dt' \omega(t'), \quad (13)$$

and making this replacement we arrive at

$$I(\omega) \sim \int_{-\infty}^{\infty} dt e^{-i\omega t} \langle e^{i\omega_T t} \rangle, \quad (14)$$

which becomes

$$I(\omega) \sim \langle \delta(\omega-\omega_T) \rangle. \quad (15)$$

Thus the line shape is written as a distribution of time-averaged frequencies, which we call the TAA to the line shape. In the next section we will discuss the choice of the averaging time.

This approach can be generalized to the case where non-Condon effects and/or rotations are important. Thus in Eq. (4) we modify the exponent as above, and in addition replace $m(t)$ with $m(T)$, to obtain

$$I(\omega) \sim \langle m(0)m(T)\delta(\omega-\omega_T) \rangle. \quad (16)$$

The line shape is now a distribution of the time-averaged frequencies weighted by the product of the transition dipole at the beginning and end of the averaging time.

Next we turn to the problem of N coupled two-state chromophores. This system has a many-body ground state $|0\rangle$, where all chromophores are in their ground states, N singly excited states, $|i\rangle$, corresponding to a single excitation on the ith chromophore with all other chromophores in their ground states, and manifolds of higher excited states. In a nonlinear spectroscopy experiment these higher manifolds may well be excited, but in an absorption experiment one can safely restrict attention to the ground state and the single-exciton manifold, and so the Hamiltonian can be written quite generally as

$$H = H_0|0\rangle\langle 0| + \sum_{ij} H_{ij}|i\rangle\langle j|, \tag{17}$$

where H_0 is the ground state Hamiltonian, H_{ii} is the Hamiltonian for local excitation on chromophore i, and H_{ij} (for $i \neq j$) are the couplings between local excitations. Note that as in Eq. (2) above, in this model there is no coupling between the ground state and the one-exciton manifold. The dipole operator is given by

$$\boldsymbol{\mu} = \sum_i \boldsymbol{\mu}_i\{|0\rangle\langle i| + |i\rangle\langle 0|\}. \tag{18}$$

Again taking a mixed quantum/classical approach, in Appendix A we derive the following semiclassical expression for the line shape:

$$I(\omega) \sim \int_{-\infty}^{\infty} dt e^{-i\omega t} \sum_{ij} \langle m_i(0) F_{ij}(t) m_j(t)\rangle, \tag{19}$$

where, of course, $m_i = \boldsymbol{\mu}_i \cdot \hat{\boldsymbol{\epsilon}}$, and $F_{ij}(t)$ are the elements of the matrix $F(t)$, which satisfies the equation

$$\dot{F}(t) = iF(t)\kappa(t), \tag{20}$$

subject to the initial condition that $F_{ij}(0) = \delta_{ij}$, and with

$$\kappa_{ij}(t) = \omega_i(t)\delta_{ij} + \omega_{ij}(t)(1 - \delta_{ij}). \tag{21}$$

Thus $\kappa(t)$ is a matrix whose diagonal elements are the fluctuating transition frequencies, $\omega_i(t)$, and whose off-diagonal elements are the fluctuating couplings $\omega_{ij}(t)$. As mentioned earlier, direct numerical integration of Eq. (20) is possible,[15,20] but when N gets large this can become intractable. Note that for a single chromophore Eq. (20) becomes a scalar equation, which can be integrated immediately, and with Eq. (19) gives Eq. (4).

We next explore some further approximations to Eq. (19). $\kappa(t)$ is a real symmetric matrix, and (at every time t) can be diagonalized by an orthogonal transformation

$$M^T(t)\kappa(t)M(t) = \lambda(t), \tag{22}$$

where $\lambda(t)$ is a diagonal matrix. In the inhomogeneous limit or static averaging approximation[10,12,26,27] $\kappa(t)$ can be replaced by its initial value, so that now

$$F(t) = e^{i\kappa(0)t}. \tag{23}$$

Using Eq. (22) the line shape can then be written as

$$I(\omega) \sim \sum_k \langle c_k(0)^2 \delta(\omega - \lambda_k(0))\rangle, \tag{24}$$

where $\lambda_k(t)$ are the eigenvalues of $\kappa(t)$, and

$$c_k(t) = \sum_i m_i(t) M_{ik}(t). \tag{25}$$

In the adiabatic approximation[15,28] the eigenvalues $\lambda_k(t)$ are assumed to be well separated from each other for all times t (and hence do not cross). In this case infinitesimal changes in the transformation matrix $M(t)$ (that is, the eigenvectors) can be neglected, and as shown in Appendix B, the line shape becomes

$$I(\omega) \sim \int_{-\infty}^{\infty} dt e^{-i\omega t} \sum_k \left\langle c_k(0)c_k(t)\exp\left[i\int_0^t dt' \lambda_k(t')\right]\right\rangle. \tag{26}$$

Note that the static averaging approximation in Eq. (24) is also easily derived from this formula.

In the TAA for the coupled case we replace $\kappa(t)$ in Eq. (20) with

$$\kappa_T = \frac{1}{T}\int_0^T dt' \kappa(t'), \tag{27}$$

and replace $m_j(t)$ by $m_j(T)$. κ_T is diagonalized by a matrix N, and as above the line shape can be written approximately as

$$I(\omega) \sim \sum_k \langle d_k(0) d_k(T) \delta(\omega - \gamma_k)\rangle, \tag{28}$$

where

$$d_k(t) = \sum_i m_i(t) N_{ik}, \tag{29}$$

and γ_k are the eigenvalues of κ_T.

Finally one can also consider the case when the couplings between chromophores are weak. In this case Oxtoby *et al.* derived an approximate result for the line shape based on the second-cumulant truncation that involves an effective frequency for the ith chromophore, given by[25]

$$\omega_i^e(t) = \omega_i(t) + \sum_{j(\neq i)} \omega_{ij}(t). \tag{30}$$

Thus the effective frequency is the bare frequency plus a sum of the couplings to all other chromophores. The second-cumulant result always produces a symmetric line shape. This result can be generalized, yielding nonsymmetric line shapes.[24] In Appendix C we provide a simple derivation of this generalization, which gives

$$I(\omega) \sim \int_{-\infty}^{\infty} dt e^{-i\omega t} \sum_i \left\langle \exp\left[i\int_0^t dt' \omega_i^e(t')\right]\right\rangle. \tag{31}$$

One might generalize this further to include non-Condon and rotational effects phenomenologically, with

$$I(\omega) \sim \int_{-\infty}^{\infty} dt e^{-i\omega t} \sum_i \left\langle m_i(0)m_i(t)\exp\left[i\int_0^t dt' \omega_i^e(t')\right]\right\rangle, \tag{32}$$

which reduces to Eq. (4) in the uncoupled case.

III. RESULTS AND DISCUSSION

We have derived some results for line shapes based on the TAA, which involve an unspecified averaging time T. To discuss how to choose T, we begin by considering the stochastic Kubo model.[18] We determine the best value of T by requiring that the linewidth from the TAA matches the exact linewidth. Surprisingly we find that, quite generally, this best value of T is given approximately by the remarkably simple formula $T = 5/\Gamma$, where Γ is the FWHM of the exact line shape. We then test the TAA on more complicated scenarios. First we consider a case where the frequency fluctuations are

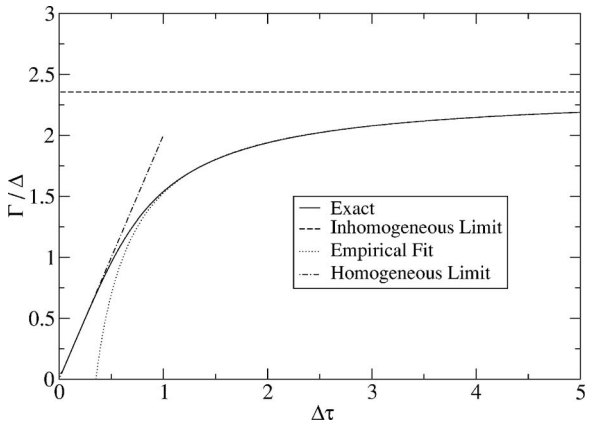

FIG. 1. Γ/Δ vs $\Delta\tau$ for the Kubo model.

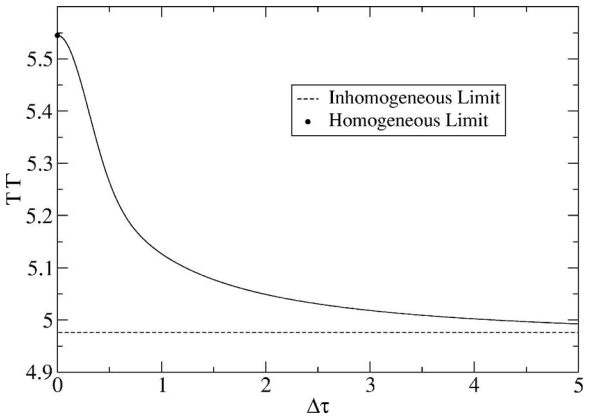

FIG. 2. $T\Gamma$ vs $\Delta\tau$ for the Kubo model.

not Gaussian and the TCF decay is nonexponential. We then consider a situation where non-Condon effects and rotations are also included. Finally, we include coupling among chromophores. We find that in all cases the TAA works well, when T is determined from $T=5/\Gamma$, and Γ is the FWHM of the exact line shape for the uncoupled chromophores within the Condon approximation and neglecting rotations. We also compare these TAA results to those from the other approximate approaches discussed above.

A. Kubo model

Kubo considered[18] a stochastic model for the fluctuating frequency, which is most conveniently taken to have zero mean. The fluctuations are described by a Gaussian random process, and the two-point TCF is given by

$$C(t)=\Delta^2 e^{-t/\tau}. \tag{33}$$

Neglecting rotations and possible non-Condon effects for the moment, in this case the line shape is given exactly by Eqs. (8) and (9). It is straightforward to show that in the inhomogeneous limit one obtains a Gaussian line shape with FWHM $\Gamma=2\sqrt{2\ln 2}\Delta\simeq 2.355\Delta$, whereas in the homogeneous limit one obtains a Lorentzian with $\Gamma=2\Delta^2\tau$. In Fig. 1 we plot Γ/Δ, determined numerically, as a function of $\Delta\tau$. One sees that for small $\Delta\tau$, $\Gamma/\Delta\simeq 2\Delta\tau$, which is valid for $\Delta\tau<0.5$, and that for large $\Delta\tau$, Γ/Δ approaches (albeit slowly) its asymptotical value of about 2.355. Finally we note that for $\Delta\tau>1$, Γ is rather well fit by

$$\frac{\Gamma}{\Delta}\simeq 2.355-\frac{0.8293}{\Delta\tau}, \tag{34}$$

which is also plotted in Fig. 1.

Since in this model $\omega(t)$ is Gaussian, so is ω_T, which means that $\langle e^{i\omega_T t}\rangle$ in Eq. (14) can be evaluated exactly. Thus for this model the TAA yields a Gaussian line shape for *any* value of T, with a FWHM given by $\Gamma=2\sqrt{2\ln 2}\sigma$, with

$$\sigma^2=\frac{2\Delta^2}{T^2}[\tau T-\tau^2+\tau^2 e^{-T/\tau}]. \tag{35}$$

As mentioned above, we simply choose T such that the linewidth of this approximate (Gaussian) line shape is identical to the width shown in Fig. 1 of the exact line shape, which can be done numerically for different values of $\Delta\tau$.

Before we show these numerical results it is interesting to consider first the homogeneous and inhomogeneous limits. In the former, since the linewidth is going to zero it is clear that $T\to\infty$. Taking the large T limit of the above and equating the resulting linewidth to $\Gamma=2\Delta^2\tau$, we find that

$$T=\frac{8\ln 2}{2\Delta^2\tau}\simeq\frac{5.545}{\Gamma}, \tag{36}$$

so that in this limit $T\Gamma=5.545$. In the inhomogeneous limit it is equally clear that $T\to 0$; expanding Eq. (35) for small T and equating the linewidth to the linewidth from Eq. (34) gives

$$T=\frac{4.976}{2\sqrt{2\ln 2}\Delta}\simeq\frac{4.976}{\Gamma}, \tag{37}$$

and so in this limit $T\Gamma=4.976$. Since in the two limits $T\Gamma$ approach two similar constants, it suggests that after finding T numerically as a function of $\Delta\tau$, on the y axis we should plot $T\Gamma$ (rather than say $T\Delta$), and these results are shown in Fig. 2. One sees that the product $T\Gamma$ is fairly constant, changing only 10% in going from $\Delta\tau=0$ to ∞. Or in other words $T\simeq 5/\Gamma$ for any value of $\Delta\tau$!

To see how well the TAA works for the line shapes themselves, in Fig. 3 we compare the exact line shape to the approximate line shape (with T chosen as in Fig. 2) for $\Delta\tau$

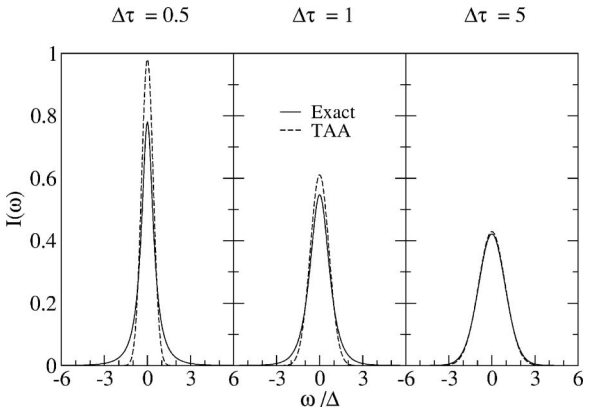

FIG. 3. Exact and time-averaging approximation line shapes for the Kubo model with several values of $\Delta\tau$.

=0.5, 1, and 5. (Note that these line shapes, and all that follow in the paper, are each normalized.) We see that for $\Delta\tau=5$ (close to the inhomogeneous limit), the TAA does an excellent job of reproducing the exact line shape. For $\Delta\tau=1$ (intermediate between homogeneous and inhomogeneous broadening), the TAA is still quite good. For $\Delta\tau=0.5$ (just into the extreme-narrowing regime according to Fig. 1), the TAA is breaking down, since it gives a Gaussian line shape while the exact result in this limit is a Lorentzian. The agreement between exact and approximate line shapes gets progressively worse as $\Delta\tau$ decreases further.

B. H_2O (uncoupled chromophores, Condon approximation, and no rotations)

In this section we will test the same approach on a more realistic model system, where the frequency fluctuations are not Gaussian, and the decay of the frequency TCF is not exponential. For such a comparison we do not have recourse to an analytical model, and so instead will consider a simple simulation model for the IR spectrum of the OH stretch regime of liquid water. In this model the fluctuating frequency of each OH stretch comes from its molecular environment (see below), and a molecular dynamics (MD) simulation of liquid water then leads to a "frequency trajectory" $\omega(t)$. Note that in real water these OH stretches are all coupled. Here, however, for illustrative purposes we will not include any coupling. In addition, in this section we will neglect non-Condon effects and rotations.

To generate the frequency trajectory we run a straightforward MD simulation of SPC/E water[34] at 300 K, with 128 molecules.[35] For each configuration we approximate each OH stretch transition frequency by

$$\omega = \{3762 - 5060(E/\text{a.u.}) - 86225(E/\text{a.u.})^2\}\ \text{cm}^{-1}, \quad (38)$$

where E is the projection of the electric field along the OH bond, evaluated at the H atom, due to the SPC/E point charges on all molecules except the one of interest within half the box length.[35] In the above a.u. signifies atomic units. This general way of parameterizing the frequency was developed by us several years ago, and the coefficients come from fitting to results from electronic structure calculations on water clusters.[19,36–38] This latest version implemented above will appear shortly.[35] Thus at each MD time step we use this equation to calculate the vibrational frequency of each OH stretch, which gives us 256 independent trajectories. For each trajectory the "exact" line shape is calculated using Eq. (6), averaging over all starting points and trajectories. The resulting line shape is shown in Fig. 4, and the FWHM is 349 cm^{-1}. We compute the TAA to the line shape from Eq. (15), choosing T from the formula derived from the Kubo model: $T=5/\Gamma$, which gives $T=76$ fs. The results for the TAA are also shown in Fig. 4. One sees that the TAA does a remarkably good job of reproducing the exact result (even though the formula for choosing T comes from the much simpler Kubo model!). For comparison in the figure we also show the distribution of frequencies, from Eq. (7). This shows that there is a modest amount of motional narrowing (actually in this case more of a shape change than a narrowing).

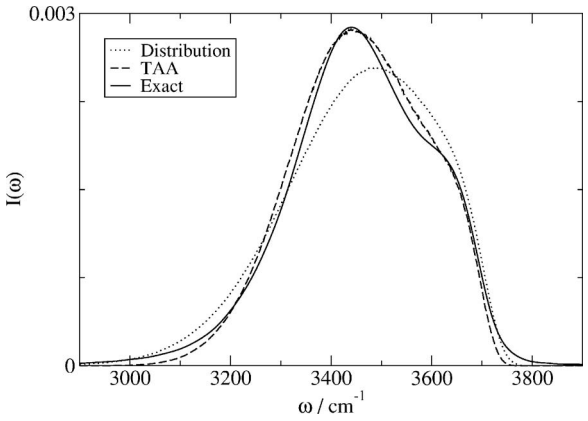

FIG. 4. OH stretch line shapes and distribution for uncoupled chromophores within the Condon approximation and neglecting rotations.

C. H_2O (uncoupled chromophores, including non-Condon effects and rotations)

In many realistic situations non-Condon effects and rotations are important, and so we want to test how well the TAA works in these cases as well. To this end we consider the same model as above, but now include non-Condon effects and rotations. The projection m of the transition dipole moment on the (light) polarization unit vector, is given approximately by[19,35,37,38]

$$m = \mu' x \hat{u}\cdot\hat{\epsilon}, \quad (39)$$

where μ' is the dipole derivative, x is the relevant matrix element of the OH stretch coordinate, and $\hat{u}$ is the unit vector of the OH bond. $\hat{u}\cdot\hat{\epsilon}$, which evolves in time due to molecular rotation, is calculated in a straightforward manner during the course of the MD simulation. Similar to Eq. (38) above, we have parameterized μ' and x,[19,35,37,38] and in the latest version we have[35]

$$\mu'/\mu'_g = 0.7112 + 75.59(E/\text{a.u.}), \quad (40)$$

and

$$x = \{0.1934 - 1.75\times 10^{-5}(\omega/\text{cm}^{-1})\}\ \text{a.u.} \quad (41)$$

μ'_g is the dipole derivative of the isolated molecule. From these three fluctuating quantities we then generate the trajectory $m(t)$, which [together with $\omega(t)$] we use to calculate the exact line shape from Eq. (4), and the result is shown in Fig. 5. The corresponding line shape from the TAA in Eq. (16), where we have used the same value of $T=76$ fs as above, is also shown in Fig. 5. As before the TAA still provides a reasonable approximation to the line shape, although not quite as good as in the absence of non-Condon effects and rotations. The inhomogenous limit from Eq. (5) involving the weighted distribution of frequencies is also shown in the figure. The comparison of this to the exact result shows the extent of motional narrowing for this system. Finally, we also show the distribution from Fig. 4, where non-Condon effects and rotations are not included. Comparison of these two distributions shows the significant effects of including these two contributions.

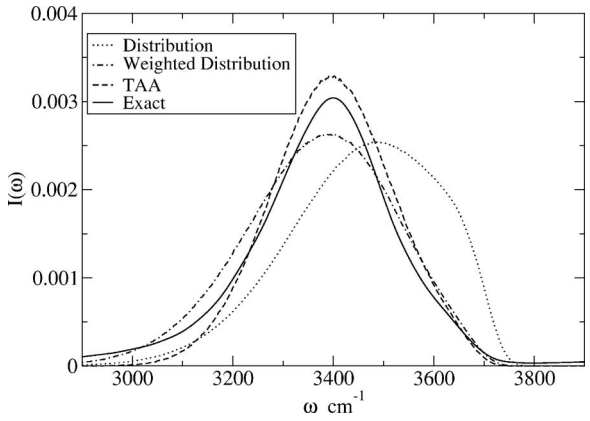

FIG. 5. OH stretch line shapes and distribution for uncoupled chromophores including non-Condon effects and rotations. For comparison we also show the distribution from Fig. 4.

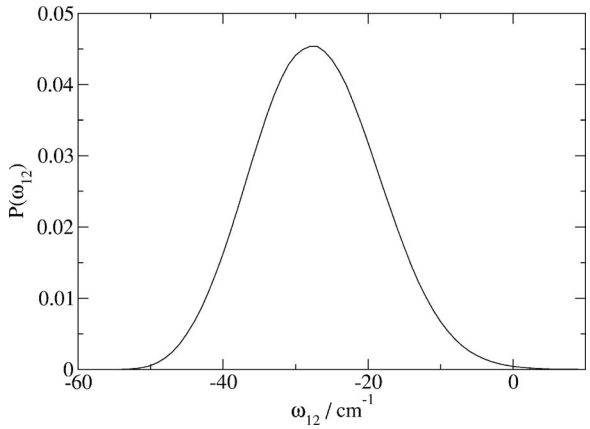

FIG. 6. Distribution of the intramolecular couplings ω_{12}. For comparison the coupling for the isolated molecule is approximately -50 cm^{-1}.

D. H_2O (coupled chromophores, Condon approximation, and no rotations)

We now consider the more challenging problem of coupled chromophores. For illustrative purposes we will again consider the water problem. In real water the two local mode chromophores on each molecule are coupled through intramolecular interactions (in the isolated molecule this coupling produces the splitting between the symmetric and asymmetric stretch frequencies of some 100 cm^{-1}), and the chromophores on different molecules are coupled through transition dipole interactions. Thus the spectroscopy of H_2O is a very challenging theoretical problem since essentially all the chromophores are coupled to each other. In order to test the TAA for coupled chromophores, we need to be able to compare to exact results. To this end we neglect the intermolecular coupling and retain only the intramolecular coupling. This means that κ in Eq. (21) is now a 2×2 matrix for each molecule, making an exact solution straightforward.

In the isolated molecule the intramolecular coupling ω_{12} is about -50 cm^{-1}. For a molecule in the liquid, however, this coupling depends strongly on the local environment. We have found that this coupling can be parameterized well by[39]

$$\omega_{12} = [\{-1789 + 23852(E_1 + E_2)/\text{a.u.}\}(x_1/\text{a.u.})(x_2/\text{a.u.}) - 1.966(p_1/\text{a.u.})(p_2/\text{a.u.})]\ \text{cm}^{-1}, \quad (42)$$

where E_1 and E_2 are the electric fields on the two hydrogen atoms of the molecule of interest, as defined previously, x_i are the relevant position matrix elements as defined in Eq. (41), and p_i are the relevant momentum matrix elements, given by

$$p_i = \{1.611 + 5.893 \times 10^{-4}(\omega_i/\text{cm}^{-1})\}\ \text{a.u.} \quad (43)$$

Thus during a simulation run for each molecule we calculate the two electric fields E_1 and E_2, the two local mode anharmonic frequencies ω_1 and ω_2, the four matrix elements x_1, x_2, p_1, and p_2, and then the intramolecular coupling ω_{12}. The distribution of intramolecular couplings is shown in Fig. 6. As seen this distribution is quite broad, and the average coupling is now roughly half of what it is for an isolated molecule. Note that for this problem the typical coupling is substantially smaller than the width of the frequency distribution.

To calculate the exact line shape for this model, we run a simulation, computing the frequency trajectory for each local mode chromophore, and the intramolecular coupling for each molecule. We then form the matrix trajectory for $\kappa(t)$ as in Eq. (21), integrate the (2×2) matrix Eq. (20) numerically for each molecule, and calculate the exact line shape from Eq. (19), averaging over all starting times and molecules. Note that in this case since we are making the Condon approximation and neglecting rotations, $m_j(t)$ are constant. The result is shown in Fig. 7. For comparison we have also shown the corresponding line shape, for the same model, but neglecting the intramolecular coupling (that is, the result in Fig. 4). This comparison shows that the coupling reduces the intensity of the shoulder at 3600 cm^{-1} and redshifts the main peak. In the same figure we also show the TAA result (for the coupled problem), from Eq. (28), using $T=76$ fs. As before we see that this approximation works quite well.

It is also interesting to compare these results to those of the effective frequency approximation in Eq. (31), which is also shown in Fig. 7. It does a reasonable job of reproducing the exact line shape, although the shoulder on the blue is too pronounced. Finally, we also show results for the adiabatic

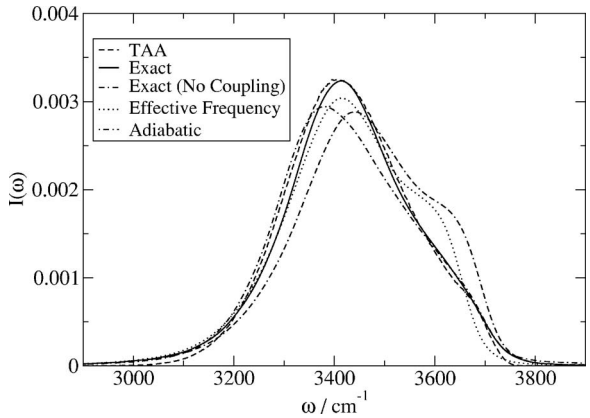

FIG. 7. OH stretch line shapes for coupled chromophores within the Condon approximation and neglecting rotations. For comparison we also show the exact line shape for uncoupled chromophores from Fig. 4.

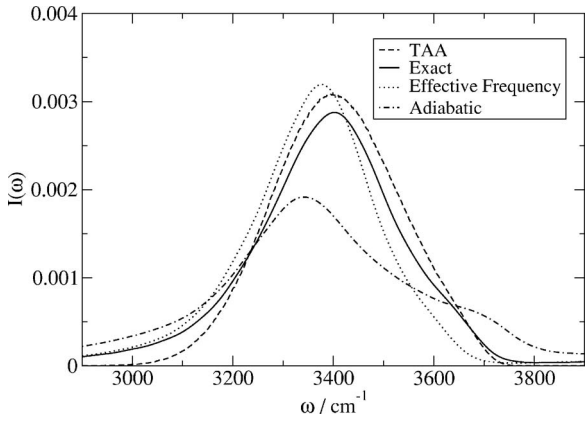

FIG. 8. OH stretch line shapes for coupled chromophores including non-Condon effects and rotations.

approximation from Eq. (26). We see that in this instance it works reasonably well, presumably because in the 2×2 case the eigenvalues never cross.

E. H_2O (coupled chromophores, including non-Condon effects and rotations)

In this final section we again consider the water problem, including non-Condon effects and rotations as in Sec. III C, and intramolecular coupling as in Sec. III D. The exact line shape is calculated using Eq. (19), and is shown in Fig. 8. The TAA, obtained from Eq. (28), using the same averaging time of $T=76$ fs, is also shown in the figure. As seen, the agreement between these two results is quite good. We also show the effective frequency approximation, now including non-Condon effects and rotations through Eq. (32), and the adiabatic approximation from Eq. (26). The former is reasonably good, while in this case the adiabatic approximation does not work well (it is unclear why its performance is significantly worse in this situation where non-Condon effects and rotations are included). In this context we note that breakdown of the adiabatic approximation has been reported recently for the similar coupled two-state problems of alanine dipeptide[16] and trialanine.[15] In any case, of the three approximations the TAA approach works the best.

IV. CONCLUDING REMARKS

We have developed a new theoretical approach to incorporating dynamical effects into line shape calculations for coupled chromophores. The approach is based on the insight that motional narrowing can be thought of as arising from a distribution of time-averaged frequencies. For the Kubo model of an isolated chromophore this time-averaging approximation (TAA) works well, for an appropriately chosen averaging time, as long as one is not in the extreme-narrowing limit (since in this case the actual line shape is a Lorentzian, while the TAA gives a Gaussian). We also tested this approach for a more realistic molecular model of an isolated OH stretch chromophore in liquid water. Guided by the Kubo model we find that we can choose the averaging time T simply from $T\simeq5/\Gamma$, where Γ is the FWHM of the actual linewidth. The model is further tested by including non-Condon effects and molecular rotations, and we find that the TAA works well, using the same value of T. We then go on to consider a model of two intramolecularly coupled OH stretch chromophores in liquid water. We find that the TAA again works well, whether or not non-Condon effects and rotations are included, still with the same averaging time T. In all cases we find that the TAA is an improvement over other simple approximate approaches.

It is probably important to reiterate that the above calculations are not intended to model vibrational spectra of real water, where at the very least one must include *intermolecular* interactions between the local mode OH stretch chromophores.[23] Rather, these models described herein were chosen so as to contain some aspects of realistic problems, where the complications of non-Condon effects, rotations, and chromophore coupling could be introduced systematically, and in all cases we could compare with exact (for the models) results.

The power of this approach is especially evident for complicated problems with many interacting chromophore, such as, for example, the OH stretch region of liquid water. In a simulation of N molecules, there will then be $2N$, or typically hundreds, of interacting chromophores. A second example is the amide I region of a protein, which again involves potentially hundreds of interacting chromophores. Our suggested implementation of the TAA for these problems involves first a simulation and semiclassical line shape calculation for the uncoupled problem, neglecting non-Condon effects and rotations. From the resulting linewidth one then obtains the appropriate averaging time. Then a second simulation is run, for the fully coupled problem (including non-Condon effects and rotations if necessary), now using the TAA to calculate the line shape.

It is clearly desirable to generalize the TAA approach to be able to describe nonlinear spectroscopy, as wonderful new information about strongly coupled chromophore systems such as water and proteins is now becoming available.[11,12,40,41] Efforts in this direction are currently underway.

ACKNOWLEDGMENT

We are grateful for support from the National Science Foundation, through Grant No. CHE-0446666.

APPENDIX A: SEMICLASSICAL LINE SHAPE FORMULA FOR COUPLED CHROMOPHORES

We begin with the general line shape formula in Eq. (1), where the absorption intensity is proportional to the Fourier transform of the quantum dipole time-correlation function, $\phi(t)$, given by

$$\phi(t)=\langle\hat{\boldsymbol{\epsilon}}\cdot\boldsymbol{\mu}(0)\boldsymbol{\mu}(t)\cdot\hat{\boldsymbol{\epsilon}}\rangle\sim\mathrm{Tr}[e^{-\beta H}\hat{\boldsymbol{\epsilon}}\cdot\boldsymbol{\mu}e^{iHt/\hbar}\hat{\boldsymbol{\epsilon}}\cdot\boldsymbol{\mu}e^{-iHt/\hbar}]. \tag{A1}$$

For the case of coupled chromophores H is given by Eq. (17), and $\boldsymbol{\mu}$ by Eq. (18). $\beta=1/kT$. The trace is over all states $|0\rangle$ and $|i\rangle$, and over the other (bath) degrees of freedom.

If the excitation energies of the singly excited states $|i\rangle$ are much larger than kT, only the ground state term survives, and so we have

$$\phi(t) \simeq \sum_{ij} \mathrm{Tr}_b[e^{-\beta H_0} m_i \langle i|e^{-i\Sigma_{kl} H_{kl}|k\rangle\langle l|t/\hbar}|j\rangle m_j e^{-iH_0 t\hbar}], \quad \text{(A2)}$$

where $m_i = \boldsymbol{\mu}_i \cdot \hat{\boldsymbol{\epsilon}}$, and Tr_b indicates a trace over bath states. Defining the bath average by $\langle \cdots \rangle_b \sim \mathrm{Tr}_b[e^{-\beta H_0} \cdots]$, and $m_i(t) = e^{iH_0 t/\hbar} m_i e^{-iH_0 t/\hbar}$, this becomes

$$\phi(t) \sim \sum_{ij} \langle m_i(0) \langle i|F(t)|j\rangle m_j(t) \rangle_b, \quad \text{(A3)}$$

where

$$F(t) = e^{i\Sigma_{kl} H_{kl}|k\rangle\langle l|t/\hbar} e^{-iH_0 t/\hbar}. \quad \text{(A4)}$$

Since in the end we will take matrix elements of F between single-exciton states [see Eq. (A3) above], in Eq. (A4) we can replace H_0 by $H_0 \Sigma_k |k\rangle\langle k|$ (using the completeness relation within the single-exciton manifold). Therefore $F(t)$ obeys the equation

$$\dot{F}(t) = iF(t)\kappa(t), \quad \text{(A5)}$$

subject to the initial condition that $F(0)=1$, and the matrix elements of $\kappa(t)$ are given by

$$\hbar \kappa_{ij}(t) = e^{iH_0 t/\hbar}(H_{ii} - H_0) e^{-iH_0 t/\hbar} \delta_{ij} + e^{iH_0 t/\hbar} H_{ij} e^{-iH_0 t/\hbar}(1 - \delta_{ij}). \quad \text{(A6)}$$

At this point we make the semiclassical approximation by replacing operators by their classical analogs, and so

$$\kappa_{ij}(t) = \omega_i(t)\delta_{ij} + \omega_{ij}(t)(1 - \delta_{ij}), \quad \text{(A7)}$$

where $\omega_i(t)$ are the fluctuating local chromophore transition frequencies, and $\omega_{ij}(t)$ are the fluctuating couplings. The quantum bath average is also replaced by the classical bath average. Thus we obtain Eqs. (19)–(21) in the body of the text.

APPENDIX B: ADIABATIC APPROXIMATION

To derive the adiabatic approximation from Eqs. (19)–(22), we define a new matrix $G(t) \equiv M^T(0)F(t)M(t)$. Note that $F(0)=1$ implies that $G(0)=1$, and that $F(t) = M(0)G(t)M^T(t)$. Eq. (20) then gives

$$M(0)\dot{G}(t)M^T(t) + M(0)G(t)\dot{M}^T(t) = iM(0)G(t)M^T(t)\kappa(t). \quad \text{(B1)}$$

The adiabatic approximation consists of setting $\dot{M}^T(t)$ to zero. That is, if as time evolves the eigenvalues $\lambda_k(t)$ are always well separated and do not cross, the eigenstates themselves change smoothly, and this change can be neglected. In this case one sees that $G(t)$ obeys the equation

$$\dot{G}(t) = iG(t)\lambda(t). \quad \text{(B2)}$$

Since $\lambda(t)$ is diagonal, the solution (subject to the initial condition) is

$$G(t) = \exp\left[i \int_0^t dt' \lambda(t') \right]. \quad \text{(B3)}$$

From this one sees that

$$F_{ij}(t) = \sum_k M_{ik}(0) \exp\left[i \int_0^t dt' \lambda_k(t') \right] M_{jk}(t), \quad \text{(B4)}$$

and then from Eq. (19) Eq. (26) follows immediately.

APPENDIX C: EFFECTIVE FREQUENCY APPROXIMATION

Next we derive Eq. (31), the semiclassical line shape result for the effective frequency. We begin by taking m_i to be constant in Eq. (19), and so

$$\phi(t) \sim \left\langle \sum_{ij} F_{ij}(t) \right\rangle, \quad \text{(C1)}$$

where $F(t)$ obeys Eqs. (20) and (21). The first of these equations can be integrated and iterated to give

$$F(t) = 1 + i\int_0^t dt' \kappa(t') - \int_0^t dt' \int_0^{t'} dt'' \kappa(t'')\kappa(t') + \cdots. \quad \text{(C2)}$$

Taking matrix elements and summing over i and j then gives

$$\sum_{ij} F_{ij}(t) = \sum_k \left(1 + i\int_0^t dt' \omega_k^e(t') - \int_0^t dt' \int_0^{t'} dt'' \omega_k^e(t'')\omega_k^e(t') + \cdots \right), \quad \text{(C3)}$$

where

$$\omega_k^e(t) = \sum_j \kappa_{kj}(t) = \omega_k(t) + \sum_{j(\neq k)} \omega_{kj}(t). \quad \text{(C4)}$$

We have used the fact that $\kappa_{ij}(t) = \kappa_{ji}(t)$ since $\omega_{ij}(t) = \omega_{ji}(t)$. Taking the average, and using the fact that classical TCFs are even in time, one obtains

$$\phi(t) \sim \sum_i \left(1 + i\int_0^t dt' \langle \omega_i^e(t') \rangle - \frac{1}{2}\int_0^t dt' \int_0^t dt'' \langle \omega_i^e(t'')\omega_i^e(t') \rangle + \cdots \right). \quad \text{(C5)}$$

These are the first three terms of an exponential expansion. (Note, however, that the next term does not continue the expansion!) An approximate resummation then yields

$$\phi(t) \sim \sum_i \left\langle \exp\left[i\int_0^t dt' \omega_i^e(t') \right] \right\rangle, \quad \text{(C6)}$$

from which follows Eq. (31). Note that a second-cumulant truncation of this result, which, as above, is valid only to second order in the effective frequency, leads to the familiar result derived first by Oxtoby *et al.*[25]

[1] S. Mukamel, *Principles of Nonlinear Optical Spectroscopy* (Oxford University Press, New York, 1995).
[2] G. R. Fleming and M. Cho, Annu. Rev. Phys. Chem. **47**, 109 (1996).
[3] J. L. Skinner and W. E. Moerner, J. Phys. Chem. **100**, 13251 (1996).
[4] E. T. J. Nibbering and T. Elsaesser, Chem. Rev. (Washington, D.C.) **104**, 1887 (2004).
[5] T. Wang, D. Du, and F. Gai, Chem. Phys. Lett. **370**, 842 (2003).
[6] I. K. Lednev, A. S. Karnoup, M. C. Sparrow, and S. A. Asher, J. Am.

Chem. Soc. **121**, 8074 (1999).
[7] P. A. Thompson, W. A. Eaton, and J. Hofrichter, Biochemistry **36**, 9200 (1997).
[8] S. Williams, T. P. Causgrove, R. Gilmanshin, K. S. Fang, R. H. Callender, W. H. Woodruff, and R. B. Dyer, Biochemistry **35**, 691 (1996).
[9] S. Mukamel and D. Abramavicius, Chem. Rev. (Washington, D.C.) **104**, 2073 (2004).
[10] J. Choi, S. Hahn, and M. Cho, Int. J. Quantum Chem. **104**, 616 (2005).
[11] P. Hamm and R. M. Hochstrasser, *Ultrafast Infrared and Raman Spectroscopy* (Dekker, New York, 2001), p. 273.
[12] Z. Ganim and A. Tokmakoff, Biophys. J. **91**, 2636 (2006).
[13] P. Mukherjee, I. Kass, I. Arkin, and M. T. Zanni, Proc. Natl. Acad. Sci. U.S.A. **103**, 3528 (2006).
[14] T. la Cour Jansen, A. G. Dijkstra, T. M. Watson, J. D. Hirst, and J. Knoester, J. Chem. Phys. **125**, 044312 (2006).
[15] R. D. Gorbunov, P. H. Nguyen, M. Kobus, and G. Stock, J. Chem. Phys. **126**, 054509 (2007).
[16] T. la Cour Jansen and J. Knoester, J. Phys. Chem. B **110**, 22910 (2006).
[17] J. G. Saven and J. L. Skinner, J. Chem. Phys. **99**, 4391 (1993).
[18] R. Kubo, Adv. Chem. Phys. **15**, 101 (1969).
[19] S. A. Corcelli and J. L. Skinner, J. Phys. Chem. A **109**, 6154 (2005).
[20] H. Torii, J. Phys. Chem. A **106**, 3281 (2002).
[21] H. Torii, M. Musso, and M. Giorgini, J. Phys. Chem. A **109**, 7797 (2005).
[22] H. Torii, J. Phys. Chem. A **110**, 4822 (2006).
[23] H. Torii, J. Phys. Chem. A **110**, 9469 (2006).
[24] K. F. Everitt, C. P. Lawrence, and J. L. Skinner, J. Phys. Chem. B **108**, 10440 (2004).
[25] D. W. Oxtoby, D. Levesque, and J.-J. Weis, J. Chem. Phys. **68**, 5528 (1978).
[26] S. Hahn, S. Ham, and M. Cho, J. Phys. Chem. B **109**, 11789 (2005).
[27] A. Belch and S. Rice, J. Chem. Phys. **78**, 4817 (1983).
[28] T. Jansen, W. Zhuang, and S. Mukamel, J. Chem. Phys. **121**, 10577 (2004).
[29] W. Zhuang, D. Abramavicius, T. Hayashi, and S. Mukamel, J. Phys. Chem. B **110**, 3362 (2006).
[30] J.-H. Choi, H. Lee, K.-K. Lee, S. Hahn, and M. Cho, J. Chem. Phys. **126**, 045102 (2007).
[31] L. Ojamäe, J. Tegenfeldt, J. Lindgren, and K. Hermansson, Chem. Phys. Lett. **195**, 97 (1992).
[32] V. Buch, J. Phys. Chem. B **109**, 17771 (2005).
[33] M. D. Stephens, J. G. Saven, and J. L. Skinner, J. Chem. Phys. **106**, 2129 (1997).
[34] H. J. C. Berendsen, J. R. Grigera, and T. P. Straatsma, J. Phys. Chem. **91**, 6269 (1987).
[35] B. Auer, R. Kumar, J. R. Schmidt, and J. L. Skinner, Proc. Natl. Acad. Sci. U.S.A. **104**, 14215 (2007).
[36] S. A. Corcelli, C. P. Lawrence, and J. L. Skinner, J. Chem. Phys. **120**, 8107 (2004).
[37] J. R. Schmidt, S. A. Corcelli, and J. L. Skinner, J. Chem. Phys. **123**, 044513 (2005).
[38] J. R. Schmidt, S. T. Roberts, J. J. Loparo, A. Tokmakoff, M. D. Fayer, and J. L. Skinner, Chem. Phys. (to be published).
[39] B. Auer and J. L. Skinner (unpublished).
[40] M. L. Cowan, B. D. Bruner, N. Huse, J. R. Dwyer, B. Chugh, E. T. J. Nibbering, T. Elsaesser, and R. D. J. Miller, Nature (London) **434**, 199 (2005).
[41] Z. Wang, Y. Pang, and D. D. Dlott, J. Phys. Chem. A **111**, 3196 (2007).